Bioresource Technology 143 (2013) 623–631

Contents lists available at SciVerse ScienceDirect

Bioresource Technology

journal homepage: www.elsevier.com/locate/biortech

Detection of algal lipid accumulation due to nitrogen limitation via dielectric spectroscopy of *Chlamydomonas reinhardtii* suspensions in a coaxial transmission line sample cell

Michael S. Bono Jr. [a], Beth A. Ahner [b], Brian J. Kirby [a,*]

[a] Sibley School of Mechanical and Aerospace Engineering, Cornell University, Ithaca, NY 14853, USA
[b] Biological and Environmental Engineering, Cornell University, Ithaca, NY 14853, USA

HIGHLIGHTS

- Dielectric spectroscopy (DES) was used to detect algal lipid accumulation.
- DES could be automated for real-time industrial algal lipid monitoring.
- A transmission line model of cell suspension permittivity was developed.
- This initial model correctly predicts observed changes in dielectric properties.

ARTICLE INFO

Article history:
Received 6 April 2013
Received in revised form 9 June 2013
Accepted 12 June 2013
Available online 20 June 2013

Keywords:
Microalgae
Lipid measurement
Nutrient limitation
Biofuel
Biodiesel

ABSTRACT

In this study, dielectric characterization of algae cell suspensions was used to detect lipid accumulation due to nitrogen starvation. Wild-type *Chlamydomonas reinhardtii* (CC-125) was cultivated in replete and nitrogen-limited conditions in order to achieve a range of lipid contents, as confirmed by Nile Red fluorescence measurements. A vector network analyzer was used to measure the dielectric scattering parameters of a coaxial region of concentrated cell suspension. The critical frequency f_c of the normalized transmission coefficient $|S_{21}^*|$ decreased with increasing lipid content but did not change with cell concentration. These observations were consistent with a decrease in cytoplasmic conductivity due to lipid accumulation in the preliminary transmission line model. This dielectric sensitivity to lipid content will facilitate the development of a rapid, noninvasive method for algal lipid measurement that could be implemented in industrial settings without the need for specialized staff and analytical facilities.

1. Introduction

Algae are considered to be one of the most promising feedstocks for biodiesel production owing to their high growth rate and decreased land requirements relative to other biofuel feedstocks (Mata et al., 2010). Many algae species produce significant biomass as lipids that can be converted to biodiesel, in addition to sugars that can be converted to ethanol or hydrogen without utilization of food crops or the conversion difficulties of woody or other lignocellulosic biomass (Jones and Mayfield, 2012). However, there are several aspects of the algal biodiesel production process which need to be improved before algal biofuels can become an economically feasible energy source (Hannon et al., 2010). In particular, the high lipid contents observed in laboratory cultures have been difficult to transfer to industrial production (Sturm and Lamer, 2011). Since biodiesel is produced from biological lipids, the ability to reliably grow algae with high lipid content at harvest will decrease the energy and monetary cost per unit of biodiesel produced (Hannon et al., 2010; Sturm and Lamer, 2011).

One of the most promising methods for increasing algal lipid content is to stress the cells by starving them of nutrients such as nitrogen (Pruvost et al., 2009) or sulfur (Cakmak et al., 2012). Nitrogen starvation in particular results in enhanced lipid accumulation in a wide variety of algae species (Mata et al., 2010; James et al., 2011). Because nitrogen starvation increases lipid levels at the cost of total growth, effective implementation involves a nitrogen-rich growth phase followed by a nitrogen-starved lipid conversion phase (Stephenson et al., 2010; Rodolfi et al., 2008). The average rate of lipid production then varies with time, resulting in an optimal harvest time. However, lipid production and growth rate are also affected by temperature (Hoffmann et al., 2010) and light exposure (Pal et al., 2011). These enviromental parameters cannot be fully controlled in an industrial setting, making the optimal harvest time variable and nondeterministic. Moreover, one of

* Corresponding author. Tel.: +1 607 255 4379; fax: +1 607 255 1222.
E-mail address: kirby@cornell.edu (B.J. Kirby).

0960-8524/$ - see front matter © 2013 Elsevier Ltd. All rights reserved.
http://dx.doi.org/10.1016/j.biortech.2013.06.040

the most promising ways to reduce the cost of algal biofuel production is to use wastewater as a culture medium (Sturm and Lamer, 2011); the resulting variation in the nutrient composition adds additional variability to algae cultivation processes. These variations necessitate the use of real-time lipid monitoring for optimal timing of harvesting and nutrient addition.

Industrial application of real-time monitoring requires improvements in lipid measurement techniques. Algal lipid content is traditionally measured by extraction and gravimetric determination, which is a complicated process requiring trained laboratory personnel and hours or days to complete (Gao et al., 2008; Gardner et al., 1985). Moreover, because the lipids are measured directly it is necessary to use large sample quantities — ~10 g dry sample mass or >1 L culture volume (Gao et al., 2008) — or accurate measurement of masses on the order of μg (Gardner et al., 1985). These attributes make extraction and gravimetric determination far too slow and complicated for real-time lipid measurement.

Faster methods to quantify algal lipid content using Nile Red staining (Gao et al., 2008; Chen et al., 2009), Fourier transform infrared spectroscopy (FTIR) (Dean et al., 2010), or liquid-state ^{1}H Nuclear Magnetic Resonance (NMR) (Davey et al., 2012) are the topics of current research, and provide answers in minutes to hours. However, each of these techniques has limitations that make them difficult to translate to an industrial setting. Nile Red can be used for quantitation of neutral algal lipids (Chen et al., 2009); however, it has variable effectiveness between algae species and organic solvents are required to penetrate the cell walls of some species (e.g., *Chlorella vulgaris*) (Chen et al., 2009; Dean et al., 2010).

FTIR of aqueous suspensions is complicated by the strong IR absorbance of water. Baseline correction is particularly difficult in cell suspensions owing to the wide variety of molecules present (Mourant et al., 2003). For these reasons, current algal lipid measurement techniques require that cells are dried before measurement (Dean et al., 2010). Liquid-state ^{1}H NMR can be used for rapid, non-invasive algal lipid measurement (Davey et al., 2012), but the high capital cost of NMR spectrometers makes this method prohibitive for industrial algal biofuel producers. All three of these methods are difficult to automate and require highly trained personnel, making them difficult to implement in industrial conditions.

Dielectric characterization methods offer a rapid (submillisecond), noninvasive, label-free method to measure cell lipid composition (Sun et al., 2007). These methods are dependent on the permittivities and conductivities of cellular components, providing insight into the composition of biological cells. Zhao et al. (2006) used dielectric spectroscopy to investigate the morphology of algae cells. Wu et al. (2005) found that *Chlorella protothecoides* cells exhibit different electrorotation spectra when grown under conditions resulting in different lipid contents, and Deng et al. (2012) used dielectrophoresis for binary separation of *Chlorella* cells with differing lipid contents. These results suggest that lipid accumulation alters the dielectric properties of algae cells. Higashiyama et al. (1999) correlated dielectric spectra with oil content in *Mortierella alpina* fungi cells, demonstrating that dielectric methods can quantitatively measure biological lipid content.

Among these techniques, dielectric spectroscopy is most suited for online automated characterization. Electrorotation and dielectrophoretic characterization experiments both require microscopic imaging and electromechanical actuation of cells on multisecond time scales (Wu et al., 2005; Deng et al., 2012; Hawkins et al., 2011). As dielectric spectroscopy only requires measuring the electrical properties of a sample over a frequency range, it is well-suited to automated measurement. Simple one-frequency capacitance measurements have been adapted for real-time biomass monitoring (Kell et al., 1990) and are already available commercially, demonstrating that dielectric probes are capable of the simple, reliable operation that real-time lipid monitoring requires. Maskow et al. (2008) used online bulk dielectric spectroscopy for monitoring lipid accumulation in yeast, suggesting that dielectric spectroscopy can be used for algal lipid monitoring. Newly developed measurement and data processing techniques allow for automated dielectric characterization of individual cells (Sun et al., 2007), paving the way for more accurate dielectric monitoring than is possible for bulk samples and facilitating characterization of more dilute cultures without preconcentration. Dielectric lipid measurement requires calibration to a direct measure of lipid content and lacks the ability to differentiate between different lipid compositions with the same electrical properties. However, it uses relatively inexpensive instrumentation, does not require highly-trained technicians or on-site lab facilities, and is well-suited to automated measurement. These results and attributes suggest that dielectric methods will allow for reliable, automated online monitoring of algal lipid content in an industrial setting.

This work describes the dielectric characterization of wild-type *Chlamydomonas reinhardtii* (CC-125) cells with a range of lipid contents induced via nitrogen starvation. James et al. (2011) and Cakmak et al. (2012) observed lipid accumulation in *Chlamydomonas reinhardtii* CC-125 under nitrogen limitation, and dielectric characterization of this strain will inform the development of lipid measurement techniques for other algae species used for biodiesel production. The normalized transmission coefficient $|S^*_{21}|$ can be measured without dyeing, lysing, or drying the cells, and requires only a vector network analyzer, an affordable, commonly available electric characterization instrument. This characterization yields a critical frequency f_c that is sensitive to cellular lipid content but unaffected by changes in cell concentration. The characterization presented in this work will facilitate the development of both more accurate models of cell dielectric properties and automated single-cell dielectric characterization methods, with the end goal of an automated, online lipid measurement system that can be used for industrial monitoring of algal biofuel feedstocks.

2. Methods

2.1. Algae culture and reagents

Wild-type *Chlamydomonas reinhardtii* (CC-125, mt+) was acquired from the Stern Laboratory at the Boyce Thompson Institute of Plant Research and maintained in liquid TAP medium cultures. TAP medium for primary cultures was acquired from Invitrogen (Grand Island, NY, USA). TAP and TAP-N media for experimental cultures were prepared based on compositions from Deng et al. (2011) and Gorman and Levine (1965). Briefly, TAP medium consisted of 10 mL 5x replete Beijerinck's solution (750 mM NH_4Cl, 35 mM $CaCl_2$, 40 mM $MgSO_4{\cdot}7H_2O$), 8.33 mL phosphate stock solution (98 mM K_2HPO_4, 54 mM KH_2PO_4), 10 mL Tris–Acetate buffer (2.00 M tris (hydroxymethyl) aminomethane, 1.75 M acetic acid), and 1 mL Hunter's trace metal solution (134 mM $Na_2EDTA{\cdot}2H_2O$, 77 mM $ZnSO_4{\cdot}7H_2O$, 184 mM H_3BO_3, 26 mM $MnCl_2{\cdot}4H_2O$, 18 mM $FeSO_4{\cdot}7H_2O$, 7 mM $CoCl_2{\cdot}6H_2O$, 5 mM $CuSO_4{\cdot}5H_2O$, 8 μM $(NH_4)_6Mo_7O_24\cdot 4H_2O$) added to milli-Q (Millipore) water for each 1 L medium. TAP-N consisted of the same formulation, with the substitution of nitrogen-free 5x Beijerinck's salt solution (750 mM NaCl, 35 mM $CaCl_2$, 40 mM $MgSO_4\cdot 7H_2O$) for replete Beijerinck's solution.

The effects of lipid accumulation on dielectric properties were investigated by inoculating 500 mL TAP medium in a 1000-mL Pyrex bottle with 1.4 mL liquid primary culture, then cultivating at 28 ± 1°C and a photon flux density of 240 ± 20 μmol/m^{2}s, supplied by adjust-

able LED light panels (color temperature 5500 K) from Fancier Photographic Equipment (Ningbo, P.R. China). After 4 days of culturing in the initial TAP medium, cells were resuspended in either fresh TAP (replete) or TAP-N (nitrogen-limited) medium and cultured for up to 2 additional days. At resuspension, cultures were centrifuged for 14 min at 3000 g, resuspended in fresh medium at the same concentration as in the original TAP medium, and grown as 100-mL batch cultures in 250-mL Pyrex bottles. The effects of cell concentration on dielectric properties were investigated by cultivating 500-mL TAP cultures at 28 ± 1°C and a photon flux density of 330± 10 μmol/m^{2}s for 4–6 days with no resuspension. In both investigations, cell concentration was quantified as the OD_{600} of the cell culture in a 1-cm-pathlength cuvette (Plastibrand 7591–65), measured using a Spectramax plus 384 spectrophotomer. The wavelength of 600 nm was selected based on measured absorption spectra of replete and nitrogen-limited cell suspensions (data not shown).

Nile red stain for fluorescence measurements was prepared by dissolving 1 mg/mL Nile red (fluorescence grade, from Sigma–Aldrich) in dimethyl sulfoxide (HPLC-grade, from Sigma–Aldrich) and storing frozen in 100-μL aliquots. Pure dimethyl sulfoxide (DMSO) was used as a negative stain control. Nile red fluorescence was measured with respect to lipid standards consisting of 2% chemically defined lipid concentrate (Gibco #11905, from Invitrogen) in deionized water, stored frozen in 1-mL aliquots.

2.2. Nile red fluorescence

Nile red fluorescence was used to quantify algal lipid content for calibration of the new dielectric measurement technique. Cell-free culture medium was obtained by centrifuging cell cultures for 14 min at 3000 g. The following 300-μL fluorescence samples were then prepared in a 96-well plate: 6 replicates per culture of cell suspension + 2 μL Nile red (denoted as "cells + NR"), cell suspension + 2 μL DMSO (denoted as "cells"), and cell-free medium (denoted as "med + NR"); 3 replicates per culture of suspending medium + 2 μL DMSO (denoted as "med"); and 3 replicates per experiment of lipid standard + 2 μL Nile red (denoted as "standard + NR") and deionized water + 2 μL Nile red (denoted as "DIW + NR"). The plate was then vortexed and incubated at room temperature for 30 min before measuring sample fluorescence using a Synergy HT BioTek plate reader. The fluorescence was measured at 5-min intervals for 30 min using an excitation filter of 530 ± 25 nm and an emission filter of 590 ± 20 nm.

The relative Nile red fluorescence, here referred to as the relative cellular lipid content (RCLC) of each algae culture was then calculated using the following equation:

$$\mathrm{RCLC} = \frac{[\mathfrak{F}(\mathrm{cells}+\mathrm{NR}) - \mathfrak{F}(\mathrm{med}+\mathrm{NR})] - [\mathfrak{F}(\mathrm{cells}) - \mathfrak{F}(\mathrm{med})]}{\langle F(\mathrm{standard}+\mathrm{NR})\rangle - \langle F(\mathrm{DIW}+\mathrm{NR})\rangle} \quad (1)$$

$\mathfrak{F}(x)$ is the mean value of the maximum fluorescence across all samples of type x and $\langle F(x)\rangle$ is the mean value of all samples of type x over time. In order to account for differences in cell concentration, the RCLC for each cell culture is divided by the OD_{600} for that culture.The resulting quantity is referred to as the normalized cellular lipid content (NCLC):

$$\mathrm{NCLC} = \frac{[\mathfrak{F}(\mathrm{cells}+\mathrm{NR}) - \mathfrak{F}(\mathrm{med}+\mathrm{NR})] - [\mathfrak{F}(\mathrm{cells}) - \mathfrak{F}(\mathrm{med})]}{\mathrm{OD}_{600}[\langle F(\mathrm{standard}+\mathrm{NR})\rangle - \langle F(\mathrm{DIW}+\mathrm{NR})\rangle]} \quad (2)$$

Since the NCLC measures the Nile red fluorescence normalized by cell concentration, it provides a measure of lipid accumulation within the algae cells. The above expression for NCLC was found to be independent of cell concentration for cells diluted up to six times, with a sample coefficient of variation of 9% (data not shown). The above protocol is modeled after that of Bittar et al. (2013).

2.3. Dielectric characterization

Algae cell samples for dielectric characterization were prepared by centrifuging algae cultures for 14 min at 3000 g, then resuspending via aspiration in fresh TAP-N medium (conductivity $\sigma = 0.27 \pm 0.01$ S/m, measured with a Mettler-Toledo SevenMulti pH/conductivity meter). Cultures used to investigate lipid accumulation (4 days culture in initial TAP followed by 0–2 days culture in fresh TAP or TAP-N) were concentrated by a factor of 37 ± 2. Cultures used to investigate the effects of cell concentration on dielectric properties (4–7 days culture in initial TAP, no resuspension) were concentrated by factors of 13, 20, 30, 40, and 50.

The concentrated cell suspensions were then placed in the coaxial transmission line sample cell shown in Fig. 1. The transmission line sample cell, adapted from Maxwell (2007), consists of a semi-rigid coaxial cable (RG401/U, acquired from Pasternack Enterprises, Irvine, CA, USA) encased in two machined copper blocks. The copper outer conductor and polytetrafluoroethylene (PTFE) dielectric were removed from a 44-mm length of the coaxial cable, exposing the inner silver-plated copper conductor and creating an annular sample region with an inner diameter of 1.64 mm and an outer diameter of 6.35 mm when the sample cell was fully assembled. Aluminum machine screws were used to close the sample injection ports on top of the device, and modeling clay (Nicole Industries, Mt. Laurel, NJ, USA) was used to seal the ends of the sample cell against leakage as seen in Fig. 1.

The dielectric scattering parameters of the algae cell suspensions in the sample cell containing were measured using a Hewlett–Packard 8753D vector network analyzer (VNA). Scattering parameters were measured at 801 frequency points log-distributed from 30 kHz to 3 GHz, with a sweep time of 3 s and 10 sweeps

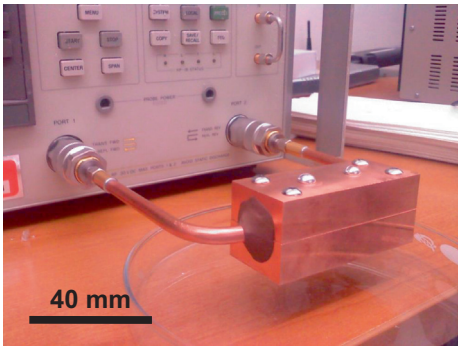

(a)

(b)

Fig. 1. Coaxial transmission line sample cell used for dielectric characterization of algae cell suspensions, shown (a) attached to the HP 8753D Vector Network Analyzer used to measure the scattering parameters of the loaded sample cell and (b) open so that the sample volume is visible. Based on a design from Maxwell, 2007.

averaged for each measurement. Scattering parameters were also measured with the same settings for the sample cell containing fresh cell-free TAP-N medium. Algae cultures were characterized using spectra of the scattering parameter S_{21}, known as the forward complex transmission coefficient.

2.4. Scattering parameter analysis and critical frequency selection

The normalized transmission coefficient $|S^*_{21}|$ was calculated for each cell suspension by dividing the measured forward complex transmission coefficient S_{21} for the cell suspension by the measured S_{21} for the suspending medium with no cells present, normalizing the resulting scattering parameter by its own value at a reference frequency f_{ref} = 10 MHz, and considering the magnitudes of the resulting frequency-dependent complex quantity. The magnitude of $|S_{21}|$ is formally known as the forward gain, but $|S^*_{21}|$ is referred to as the normalized transmission coefficient for simplicity and to emphasize its physical nature of measuring the extent to which algae cell suspensions permit transmission of electromagnetic waves.

The critical frequency f_c of $|S^*_{21}|$ for each algae culture was determined by smoothing $|S^*_{21}|$ using a 2nd-degree Savitzky–Golay filter with a 30–point span, then numerically differentiating the smoothed spectrum and selecting the frequency with the minimal first derivative between 100 kHz and 1.25 MHz, corresponding to an inflection point in $|S^*_{21}|$ in that frequency range. MATLAB R2012a was used for all data analysis.

3. Theory

3.1. Suspension permittivity

Dielectric characterization of biological cells measures the interfacial polarization that occurs when an electric field is applied to a heterogeneous suspension. In a cell suspension, the cell components and suspending medium are lossy dielectrics: they attenuate electric fields via both polarization of the individual molecules and conduction of ions or electrons within each material. Hence, each component of the suspension is characterized by both an electrical permittivity ϵ, the degree to which it attenuates an electric field via polarization, and an electrical conductivity σ, the degree to which it allows passage of ions or electrons under application of an electric field. The presense of both polarization and conduction results in a frequency-dependent dielectric response which can be evaluated by combining the permittivity and conductivity into a frequency-dependent complex permittivity $\epsilon^* = \epsilon + \sigma/j\omega$, where $j = \sqrt{-1}$ and $\omega = 2\pi f$ is the angular frequency of the applied electric field.

When an electric field is applied to a particle suspension, interfacial polarization at the particles' surfaces will result in an effective suspension permittivity ϵ^*_{susp} that is a function of the complex permittivities of the particles (ϵ^*_p) and the suspending medium (ϵ^*_m). This change in permittivity occurs owing to the modification of the electric field near the particles, which will resemble that formed by the presence of electric dipoles. If the suspension is sufficiently dilute that these induced dipoles do not interact, then the effective suspension permittivity can be described by Maxwell's mixture equation (Kirby, 2010):

$$\epsilon^*_{susp} = \epsilon^*_m\left[\frac{1+2\phi f^*_{CM}}{1-\phi f^*_{CM}}\right], \qquad f^*_{CM} = \frac{\epsilon^*_p - \epsilon^*_m}{\epsilon^*_p + 2\epsilon^*_m} \tag{3}$$

where ϕ is the volume fraction of the particles and f^*_{CM} is the complex Clausius–Mossotti factor, which describes the difference in dielectric properties between particles with complex permittivity ϵ^*_p and a suspending medium with complex permittivity ϵ^*_m.

Heterogeneous particles such as biological cells do not have a single ϵ^*_p; however, their behavior can be described by an effective ϵ^*_p that accounts for the morphology and electrical properties of the different cellular components. One simple but effective method to model the interfacial polarization within the cell is to treat it as a spherically symmetrical particle, with a cytoplasm surrounded by a discrete number of shells corresponding to different components of the cell membrane and wall. For a spherical particle consisting of a core with radius R_{core} and complex permittivity ϵ^*_{core} surrounded by a shell with radius R_{shell} and complex permittivity ϵ^*_{shell}, the effective permittivity ϵ^*_{eff} of the particle is (Kirby, 2010)

$$\epsilon^*_{p,eff} = \epsilon^*_{shell}\left[\frac{\frac{R^3_{shell}}{R^3_{core}} + 2f^*_{CM}}{\frac{R^3_{shell}}{R^3_{core}} - f^*_{CM}}\right], \qquad f^*_{CM} = \frac{\epsilon^*_{core} - \epsilon^*_{shell}}{\epsilon^*_{core} + 2\epsilon^*_{shell}} \tag{4}$$

This relationship can be applied iteratively to model particles with multiple shells, with the effective permittivity $\epsilon^*_{p,eff}$ up to a given shell used as ϵ^*_{core} for the next core–shell interface. In the initial model, each *Chlamydomonas reinhardtii* cell is described as a spherical cytoplasm with complex permittivity ϵ^*_{cyt} surrounded by shells corresponding to the plasma membrane (with complex permittivity ϵ^*_{mem}) and the cell wall (with complex permittivity ϵ^*_{wall}), as shown in Fig. 2(a). More accurate modeling could be achieved by including the ellisoidal shape of the cell and the multiple components of the cell wall and cytoplasm (Goodenough and Heuser, 1985; Hawkins et al., 2011).

3.2. Transmission line model

In this study, the dielectric properties of each algae cell suspension are characterized by measuring the transmission coefficient S_{21} of a transmission line containing the cell suspension. Transmission line characterization enables measurement of dielectric properties over a wide frequency range, since transmission line analysis accounts for changes in the phase of the applied electric field over the sample geometry. This allows for characterization even when the wavelength of the applied signal approaches the sample size.

A transmission line can be characterized by measuring its scattering parameter matrix S, a complex matrix representation of the portions of an incoming electromagnetic wave that are reflected and transmitted by the transmission line. Geometric differences in the electrical properties of the transmission line materials result in partial reflection of incident electromagnetic waves, making scattering parameters an indirect measurement of the complex permittivity ϵ^*_{susp} of a volume of cell suspension contained within the sample cell as shown in Fig. 2(b).

A uniform two-conductor transmission line is a distributed circuit characterized by its characteristic impedance Z_0, complex propagation constant γ, and length ℓ. Z_0 and γ are determined by the electrical properties of the transmission line components as encapsulated in four differential circuit parameters: the series resistance R per unit length, the series inductance L per unit length, the shunt conductance G per unit length, and the shunt capacitance C per unit length (Pozar, 2012):

$$Z_0 = \sqrt{\frac{R+j\omega L}{G+j\omega C}}, \qquad \gamma = \sqrt{(R+j\omega L)(G+j\omega C)} \tag{5}$$

In a coaxial transmission line sample cell like the one shown in Fig. 1, R corresponds to the surface resistance of the electrodes and L, G, and C correspond to sample volume magnetization, conduction, and polarization, respectively. For a uniform coaxial transmission line with inner radius a, outer radius b, and electrode surface conductance R_s containing a general lossy material with

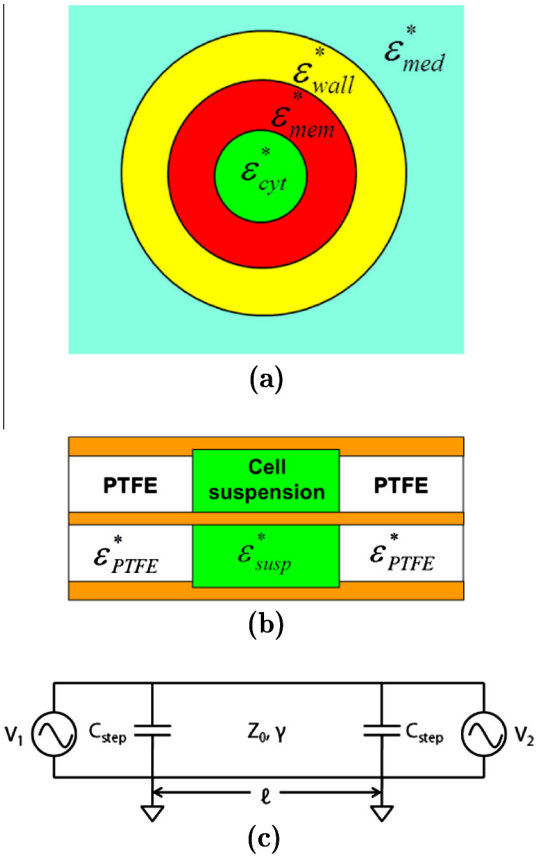

Fig. 2. (a) Multishell model of cell morphology. $\epsilon^*_{cyt}, \epsilon^*_{mem}, \epsilon^*_{wall}$, and ϵ^*_{med} are the complex permittivities of the cytoplasm, plasma membrane, cell wall, and suspending medium, respectively, as defined in Section 3.1. (b) Geometry of algae cell suspension within coaxial transmission line sample cell used for dielectric characterization (shown in Fig. 1). (c) Circuit representation of the coaxial transmission line sample cell. Variables defined in Section 3.2.

complex permittivity ϵ^* and magnetic permeability μ, the values of R, L, G, and C are (Pozar, 2012)

$$R = \frac{R_s}{2\pi}\left(\frac{1}{a}+\frac{1}{b}\right) \quad L = \frac{\mu}{2\pi}\ln\frac{b}{a} \tag{6}$$

$$G = \frac{-2\pi\omega\Im m[\epsilon^*]}{\ln b/a} \quad C = \frac{2\pi\Re e[\epsilon^*]}{\ln b/a} \tag{7}$$

note minus sign in eqn for G added after publication

Transmission lines may contain a combination of discrete and distributed elements. In the coaxial transmission line sample cell used in this study, the transition from the PTFE dielectric to the cell suspension is accompanied by a change in outer conductor diameter, as seen in Fig. 1. This change in diameter results in a shunt step capacitance C_{step} before and after the coaxial transmission line, as shown in the circuit diagram in Fig. 2(c). This step capacitance is a function of the geometry of the transition and the permittivities of the two dielectrics. Numerical analysis of the electromagnetic propogation modes at the transition yields the formula (Maxwell, 2007):

$$C_{step} = \pi a \epsilon_{r,1}\left[\frac{\epsilon^*_2}{\pi}\left(\frac{\alpha^2+1}{\alpha}\ln\frac{1+\alpha}{1-\alpha} - 2\ln\frac{4\alpha}{1-\alpha^2}\right) + \left(4.12\times10^{-13}\right)(0.8-\alpha)(\tau-1.4)\right] \text{F}, \tag{8}$$

$$\text{where} \quad \alpha = \frac{b_1-a}{b_2-a}, \quad \tau = \frac{b_2}{a},$$

a is the inner conductor radius, b_1 and b_2 are the outer conductor radius before and after the transition, respectively, $\epsilon_{r,1}$ is the relative permittivity of the dielectric before the transition, and ϵ^*_2 is the complex permittivity of the dielectric after the transition. Thus, the full circuit for the transmission line sample cell (Fig. 2(c)) consists of two shunt capacitances C_{step} on either end of a uniform coaxial transmission line with length ℓ, characteristic impedance Z_0, and complex propagation constant γ as defined above.

Transmission lines are characterized by measuring the scattering parameters of the transmission line. The scattering parameter matrix describes the portions of an incoming electromagnetic wave that are reflected and transmitted by a network. For a two-port network such as a single transmission line, the scattering parameter matrix is defined as (Pozar, 2012)

$$\begin{bmatrix} V_1^- \\ V_2^- \end{bmatrix} = \begin{bmatrix} S_{11} & S_{12} \\ S_{21} & S_{22} \end{bmatrix} \begin{bmatrix} V_1^+ \\ V_2^+ \end{bmatrix} \tag{9}$$

where V_i^- denotes the amplitude of a voltage wave exiting port i and V_j^+ denotes the amplitude of a voltage wave incident on port j. The diagonal components S_{11} and S_{22} of the scattering parameter matrix correspond to the forward and reverse reflection coefficients, respectively, and the off-diagonal components correspond to transmission coefficients. The dielectric characterization method described here utilizes the forward transmission coefficient S_{21}, which is the portion of an electromagnetic wave incident at port 1 which is transmitted to port 2. Because reflection of incident electromagnetic waves arises from differences in electrical properties between the cell suspension and the rest of the coaxial cable, S_{21} is a measure of the similarity in electrical properties between the cell suspension and the PTFE dielectric in the remainder of the coaxial cable.

Measured scattering parameters can be related to sample material properties through the use of the transmission matrix, also known as the ABCD matrix. Whereas the scattering parameter matrix relates incident, reflected, and transmitted waves, the ABCD matrix relates the total voltage and current at ports 1 and 2 of a two-port network (Pozar, 2012):

$$\begin{bmatrix} V_1 \\ I_1 \end{bmatrix} = \begin{bmatrix} A & B \\ C & D \end{bmatrix} \begin{bmatrix} V_2 \\ I_2 \end{bmatrix} \tag{10}$$

For the ABCD matrix, I_1 is defined as the current flowing into port 1, whereas I_2 is defined as the current flowing out of port 2. This definition allows for analysis of a series of N network elements by defining an ABCD matrix for each element i and multiplying them together to determine the ABCD matrix for the entire network. The ABCD matrix for the sample cell circuit shown in Fig. 2(c) is the product of the ABCD matrices for a shunt capacitance C_{step}; a transmission line with characteristic impedance Z_0, complex propagation constant γ, and length ℓ; and another shunt capacitance C_{step} (Pozar, 2012):

$$\begin{bmatrix} A & B \\ C & D \end{bmatrix}_{\text{sample}} = \begin{bmatrix} 1 & 0 \\ j\omega C_{step} & 1 \end{bmatrix} \begin{bmatrix} \cosh\gamma\ell & Z_0\sinh\gamma\ell \\ Z_0^{-1}\sinh\gamma\ell & \cosh\gamma\ell \end{bmatrix} \begin{bmatrix} 1 & 0 \\ j\omega C_{step} & 1 \end{bmatrix} \tag{11}$$

The ABCD matrix can then be converted to a theoretical scattering parameter matrix for comparison with measured scattering parameters (Pozar, 2012).

In order to predict the measured scattering parameters for a sample with complex permittivity ϵ^*_{susp}, the complex permittivity is first used to define Z_0, γ, and C_{step}. These transmission line properties can then be used to define an ABCD matrix for the sample cell, which can be converted to the expected scattering parameters for comparison with measurements.

3.3. Parameter selection

In order to anticipate expected changes in measured scattering parameters due to lipid accumulation, typical electrical properties of cellular components were used to calculate theoretical values of $|S_{21}^*|$ for different degrees of lipid accumulation. Depending on the species of algae, lipid accumulation during nitrogen starvation may be accompanied by changes in other morphological and biochemical properties such as cell size (James et al., 2011), membrane properties (Wu et al., 2005), and starch content (Dean et al., 2010; Cakmak et al., 2012). Since this model is intended for anticipation of observed dielectric sensitivity rather than complete prediction of measured spectra, only the property changes directly due to cytoplasmic lipid accumulation were incorporated into this model, with all other cell properties held constant.

Electrical properties were selected from previously measured values for biological cells, using values for algae when possible. Geometrically, the *Chlamydomonas reinhardtii* cell were modeled as 14-μm-diameter spherical cytoplasms surrounded by a 4.5-nm-thick plasma membrane (Hawkins et al., 2011) and a 165-nm-thick cell wall (Goodenough and Heuser, 1985). Lipid accumulation was modeled as changes in the properties of the cytoplasm owing to the increased presence of lipid deposits (Higashiyama et al., 1999). The cytoplasm was modeled as having a relative permittivity of 60 (Hawkins et al., 2011; Sun et al., 2007) and a conductivity σ_{cyt} that decreased with lipid accumulation, with values of 1200, 400, and 200 mS/m selected for cells with low, intermediate, and high lipid content, respectively, based on inferred values from Higashiyama et al. (1999). This theoretical variation of cellular lipid content is shown in Fig. 3(c). For theoretical variation of cell concentration (Fig. 3(d)), σ_{cyt} was held constant at 1200 S/m.

The membrane relative permittivity and conductivity were taken to be 2.3 and 10 μS/m, respectively, based on dielectric characterization of *Escherichia coli* cells (Hawkins et al., 2011). The cell wall conductivity was modeled as 50 mS/m (measured by Wu et al. (2005) for *Chlorella protothecoides*), and the cell wall relative permittivity was taken as 60 in order to conform with measured spectra. The suspending medium relative permittivity was taken to be 80 (that of pure water), with a conductivity equal to the measured value of 0.27 S/m. Cell volume fraction ϕ was varied from 0.1 to 0.2 for theoretical variation of cell concentration (Fig. 3(d)) and held constant at 0.1 for theoretical variation of cellular lipid content.

4. Results and discussion

4.1. Scattering parameters of algae suspensions

As seen in typical $|S_{21}^*|$ spectra (Fig. 3(a)), the critical frequencies f_c of cell suspensions with higher normalized cellular lipid contents (NCLCs) due to nitrogen starvation are lower than the critical frequency of a suspension of cells with lower lipid content. This is

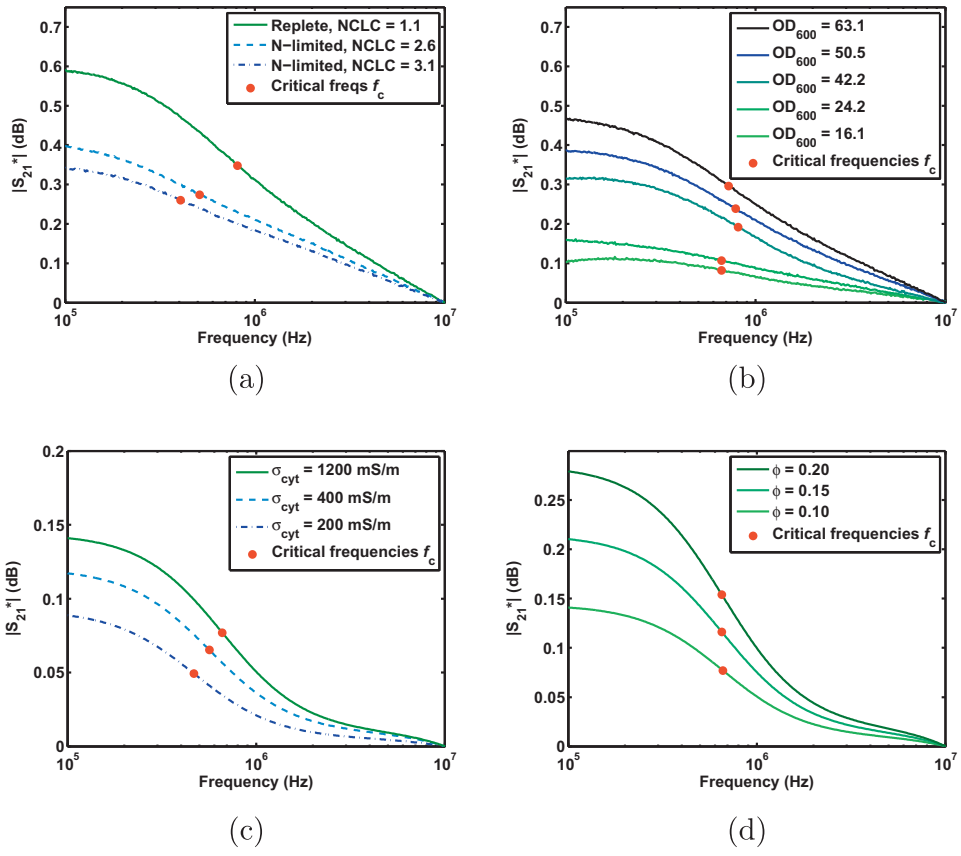

Fig. 3. (a) Measured normalized transmission coefficients $|S_{21}^*|$ and critical frequencies f_c for *Chlamydomonas reinhardtii* cells suspended in TAP-N medium after culturing in replete or N-limited conditions for 2 days. NCLC is the normalized cellular lipid content as defined in Section 2.2. (b) Measured normalized transmission coefficients $|S_{21}^*|$ and critical frequencies f_c for *Chlamydomonas reinhardtii* cells suspended in TAP-N medium at different concentrations after culturing in TAP medium for 4–6 days. Extrapolated OD_{600} is equal to the measured OD_{600} of the cell suspension multiplied by the factor of concentration. (c) Theoretical normalized transmission coefficients $|S_{21}^*|$ and critical frequencies f_c for cells modeled as described in Section 3.1 with a constant volume fraction $\phi = 0.10$, cytoplasmic conductivities from 200–1200 mS/m, and other properties as defined in Section 3.3. (d) Theoretical normalized transmission coefficients $|S_{21}^*|$ and critical frequencies f_c for cells modeled as described in Section 3.1 with volume fractions ϕ from 0.10 to 0.20, a constant cytoplasmic conductivity $\sigma_{cyt} = 1200$ mS/m, and other properties as defined in Section 3.3.

the expected effect according to the theoretical transmission line model, as seen in Fig. 3(c).

However, the critical frequency f_c remained relatively constant (sample mean ± standard deviation = 736 ± 61 kHz, N = 9) for cells cultivated in replete medium and concentrated to different degrees before dielectric characterization, as seen in the representative spectra in Fig. 3(b). There was some variation in f_c between cultures (presumably due to slight differences in lipid content and other cellular properties) but very little change for the same culture at different concentrations and no significant non-zero slope in f_c with respect to OD_{600} over all cultures (Fig. 5(a)). This is also in agreement with the theoretical model (Fig. 3(d)), which predicts that f_c will be independent of cell concentration. These results indicate that dielectric characterization yields a critical frequency that is sensitive to algal lipid content and independent of cell concentration.

4.2. Effects of nitrogen starvation

As seen in Fig. 4, cells resuspended in nitrogen-limited medium exhibit greater normalized lipid content but decreased growth relative to cells resuspended in fresh replete medium, which grow significantly but actually exhibit a slight decrease in measured NCLC. This observed decrease suggests that cells grown to late-log stage in replete medium undergo a certain degree of lipid accumulation due to the reduced nutrients in the growth medium; this lipid accumulation is reversed once the cells are presented with a fresh source of nutrients. This is similar to the lipid accumulation and decreased growth observed by James et al. (2011) and Cakmak et al. (2012) for *Chlamydomonas reinhardtii* CC-125 during nitrogen starvation. The measured critical frequency f_c of the normalized transmission coefficient $|S_{21}^*|$ decreases with resuspension time in N-limited medium and increases slightly with resuspension time in replete medium, consistent with the trend of decreased f_c due to lipid accumulation shown in Fig. 3(a).

4.3. Comparison with transmission line model

When the measured critical frequencies f_c shown in Fig. 4 are plotted with respect to the measured normalized lipid content (NCLC) for each algae sample, the critical frequency decreases with increasing lipid content as shown in Fig. 5(b). This is consistent with the trend predicted by the theoretical model (Fig. 3(c)), in which lipid accumulation decreases the cells' cytoplasmic conductivity and thus the critical frequency f_c of $|S_{21}^*|$ for the cells in suspension.

Moreover, the measured decrease in f_c is greater than that predicted for lipid accumulation alone. This is because the initial model considers only lipid accumulation and not other concurrent changes in cell morphology during nitrogen starvation. In reality, *Chlamydomonas reinhardtii* cells accumulating lipids due to nitrogen starvation also increase in size (Dean et al., 2010). Other algae species have been observed to exhibit changes in the cell wall and plasma membrane (Wu et al., 2005) during lipid accumulation, suggesting the possibility of additional morphological and biochemical changes which have not yet been observed in *Chlamydomonas reinhardtii*. Further characterization of changes in microalgae cells during nitrogen starvation and other environmental stresses will enable a more detailed model which more accurately predicts changes in f_c during lipid accumulation.

In addition, the relaxation in $|S_{21}^*|$ occurs over a wider frequency range in the measured spectra than in the theoretical spectra. Cells in culture will exhibit a range of sizes and lipid contents (Berberoglu et al., 2008; Velmurugan et al., 2013). This polydispersity will result in a distribution of relaxation times τ_{cyt}, causing the measured relaxation to occur over a wider frequency range than that predicted by

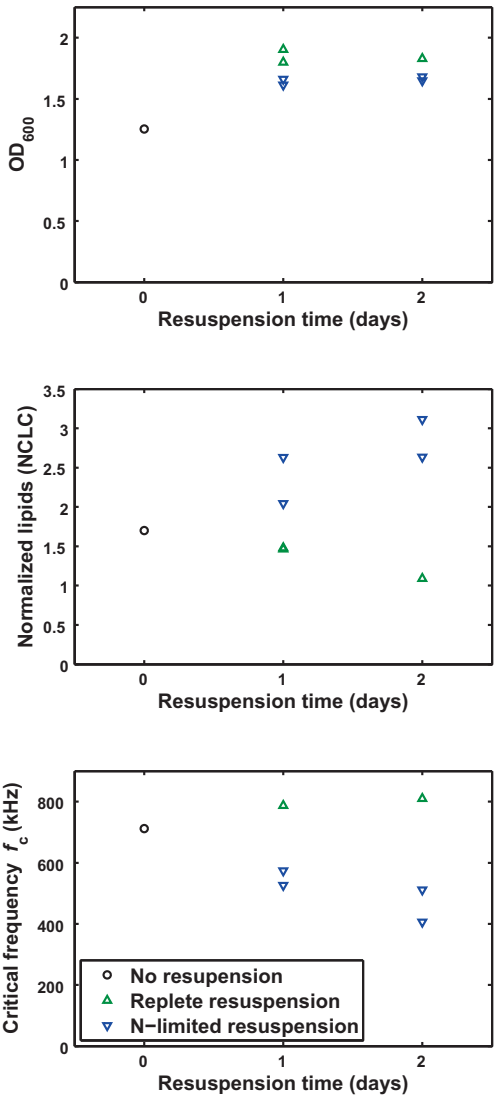

Fig. 4. Measured OD_{600} (top), normalized cellular lipid content NCLC (middle), and critical frequency f_c (bottom) for *Chlamydomonas reinhardtii* cultures as a function of resuspension time in replete (TAP) or nitrogen-limited (TAP-N) media. Procedures for measuring OD_{600}, NCLC, and f_c are described in Sections 2.1, 2.2, and 2.4, respectively.

the current monodisperse suspension model (Asami, 2002). In addition, *Chlamydomonas reinhardtii* cells contains more components than accounted for in the initial two-shell cell model (Goodenough and Heuser, 1985). This will result in more interfaces and more relaxations, which may be sufficiently close to resemble one extended relaxation (Zhao et al., 2006). A more detailed model of *Chlamydomonas* cell morphology would result in an improved ability to estimate the electrical properties of algal cell components.

Future work will focus on investigating the distribution of lipid content and size in cells over a wide range of lipid accumulation in order to account for both morphological changes due to nutrient limitation and polydispersity within cell cultures. This will inform the development of a more accurate model for dielectric properties of algae cell suspension, facilitating more accurate lipid measurement and a better understanding of lipid accumulation due to nutrient limitation.

4.4. Estimation of measurement precision

This study does not compare f_c to a direct measure of algal lipid content; however, the proportionality of Nile Red fluorescence to

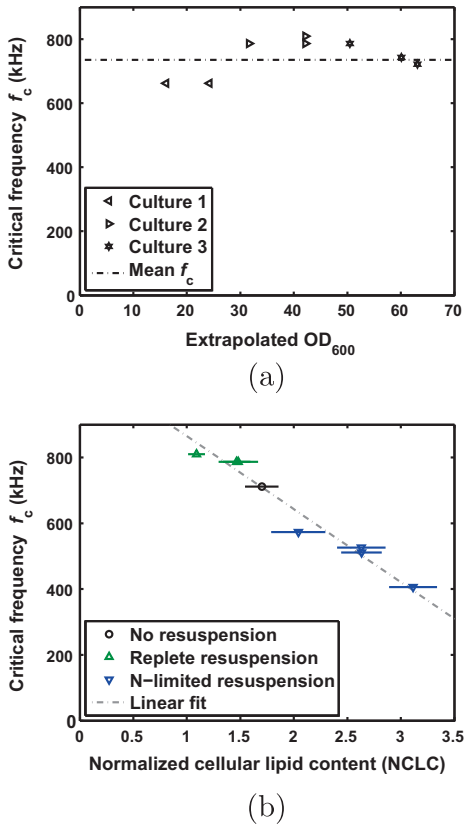

Fig. 5. (a) Measured critical frequencies f_c for *Chlamydomonas reinhardtii* cells suspended in TAP-N medium at different concentrations after culturing in TAP medium for 4–6 days, plotted as a function of extrapolated OD_{600}. (b) Critical frequencies f_c as defined in Section 2.4 plotted with respect to normalized cellular lipid content (NCLC) as defined in Section 2.2 for *Chlamydomonas reinhardtii* cells suspended in TAP-N medium after culturing in replete or N-limited conditions. NCLC error bars are ±3 standard errors of the mean, calculated via propagation of error from the fluorescence replicates described in section 2.2. Linear fit is NCLC = 4.8970–0.0045f_c for f_c measured in kHz.

neutral lipid content (Chen et al., 2009) allows comparison to previous direct measurements of lipid accumulation in *Chlamydomonas reinhardtii* CC-125 in order to estimate the measurement precision of the described dielectric characterization technique. James et al. (2011) measured lipid content of *Chlamydomonas reinhardtii* CC-125 as a percentage of cellular dry weight (%DW) and found that cells cultured for four days in TAP medium were 8.9%DW fatty acids, whereas cells cultured for four days in TAP-N medium were 12.9%DW fatty acids. Because their TAP culture was grown to stagnation, it forms an analog to the cells in this study immediately before resuspension (NCLC = 1.68). Their TAP-N culture represents an upper limit of possible lipid content for CC-125, corresponding to the maximum measured NCLC of 5.35 for cells after three days of starvation (data not shown). The observed increase of 3.67 in NCLC over three days of starvation can then be said to correspond to approximately a 4%DW increase in lipids.

As described in Section 4.3, the current model for cell permittivity does not fully describe the observed relationship between f_c and NCLC. A linear regression of NCLC as a function of f_c over the measured f_c range yields the empirical calibration curve NCLC = 4.8970–0.0045f_c for f_c measured in kHz, with $r^2 = 0.959$ and a standard estimate error $\sigma_{est} = 0.154$. If the increase in NCLC of 3.67 over three days of nitrogen starvation is taken to correspond to a lipid increase of 4%DW, then the precision of the empirical calibration curve is approximately 0.17%DW in the range of lipid contents encountered within two days of starvation. Future work will allow direct measurement of lipid content precision and deconvolution from other cellular changes in order to compliment the rough estimates presented in this study.

5. Conclusions

Dielectric spectroscopy is a rapid, noninvasive method for algal lipid measurement that could be implemented in industrial settings without the need for specialized staff and analytical facilities. In this study, dielectric characterization of wild-type *Chlamydomonas reinhardtii* cell suspensions was used to detect lipid accumulation due to nitrogen starvation. The critical frequency f_c of the normalized transmission coefficient $|S^*_{21}|$ decreased with increasing cellular lipid content (as measured by Nile red fluorescence) but did not change with cell concentration, making it a promising marker for measuring algal lipid content.

Acknowledgements

This work made use of the Cornell Center for Nanoscale Systems (NSF EEC-0117770, 0646547 and NYSTAR C020071), Cornell Center for Materials Research (NSF DMR-0520404, DMR-1120296), Cornell Nanobiotechnology Center, and Emerson Manufacturing Teaching Lab. MSB was supported by the Department of Defense (DoD) through the National Defense Science and Engineering Graduate Fellowship (NDSEG) Program. The authors would like to acknowledge Lawrence Bonassar for use of the plate reader, Zackary Johnson (Duke University) for the detailed Nile red protocol, and Kurt Rhoads (Case Western Reserve University), Lubna Richter, Michael Walsh, Joseph Sullivan, Susanna Kahn, Matthew Fulghum (Pennsylvania State University), and members of the Cornell Micro/Nanofluidics Laboratory for technical assistance and helpful discussions.

References

Asami, K., 2002. Characterization of heterogeneous systems by dielectric spectroscopy. Progress in Polymer Science 27, 1617–1659.
Berberoglu, H., Pilon, L., Melis, A., 2008. Radiation characteristics of *Chlamydomonas reinhardtii* CC125 and its truncated chlorophyll antenna transformants tla1, tlaX and tla1-CWD. International Journal of Hydrogen Energy 33, 6467–6483.
Bittar, T.B., Lin, Y., Sassano, L.R., Wheeler, B.J., Brown, S.L., Cochlan, W.P., Johnson, Z.I., 2013. Carbon allocation under light and nitrogen resource gradients in two model marine phytoplankton. Journal of Phycology. http://dx.doi.org/10.1111/jpy.12060.
Cakmak, T., Angun, P., Demiray, Y.E., Ozkan, A.D., Elibol, Z., Tekinay, T., 2012. Differential effects of nitrogen and sulfur deprivation on growth and biodiesel feedstock production of *Chlamydomonas reinhardtii*. Biotechnology and Bioengineering 109, 1947–1957.
Chen, W., Zhang, C., Song, L., Sommerfeld, M., Hu, Q., 2009. A high throughput Nile red method for quantitative measurement of neutral lipids in microalgae. Journal of Microbiological Methods 77, 41–47.
Davey, P.T., Hiscox, W.C., Lucker, B.F., O'Fallon, J.V., Chen, S., Helms, G.L., 2012. Rapid triacylglyceride detection and quantification in live micro-algal cultures via liquid state ^{1}H NMR. Algal Research 1, 166–175.
Dean, A.P., Sigee, D.C., Estrada, B., Pittman, J.K., 2010. Using FTIR spectroscopy for rapid determination of lipid accumulation in response to nitrogen limitation in freshwater microalgae. Bioresource Technology 101, 4499–4507.
Deng, X., Fei, X., Li, Y., 2011. The effects of nutritional restriction on neutral lipid accumulation in Chlamydomonas and Chlorella. African Journal of Microbiology Research 5, 260–270.
Deng, Y.L., Chang, J.S., Juang, Y.J., 2012. Separation of microalgae with different lipid contents by dielectrophoresis. Bioresource Technology. http://dx.doi.org/10.1016/j.biortech.2012.11.046.
Gao, C., Xiong, W., Zhang, Y., Yuan, W., Wu, Q., 2008. Rapid quantitation of lipid in microalgae by time-domain nuclear magnetic resonance. Journal of Microbiological Methods 75, 437–440.
Gardner, W.S., Frez, W.A., Cichocki, E.A., Parrish, C.C., 1985. Micromethod for lipids in aquatic invertebrates. Limnology and Oceanography 30, 1099–1105.
Goodenough, U.W., Heuser, J.E., 1985. The Chlamydomonas cell wall and its constitutent glycoproteins analyzed by the quick-freeze, deep-etch technique. The Journal of Cell Biology 101, 1550–1568.
Gorman, D.S., Levine, R., 1965. Cytochrome f and plastocyanin: their sequence in the photosynthetic electron transport chain of *Chlamydomonas reinhardii*.

Proceedings of the National Academy of Sciences of the United States of America 54, 1665–1669.
Hannon, M., Gimpel, J., Tran, M., Rasala, B., Mayfield, S., 2010. Biofuels from algae: challenges and potential. Biofuels 1, 763–784.
Hawkins, B.G., Huang, C., Arasanipalai, S., Kirby, B.J., 2011. Automated dielectrophoretic characterization of *Mycobacterium smegmatis*. Analytical Chemistry 83, 3507–3515.
Higashiyama, K., Sugimoto, T., Yonezawa, T., Fujikawa, S., Asami, K., 1999. Dielectric analysis for estimation of oil content in the mycelia of *Mortierella alpina*. Biotechnology and Bioengineering 65, 537–541.
Hoffmann, M., Marxen, K., Schulz, R., Vanselow, K.H., 2010. TFA and EPA productivities of *Nannochloropsis salina* influenced by temperature and nitrate stimuli in turbidostatic controlled experiments. Marine Drugs 8, 2526–2545.
James, G.O., Hocart, C.H., Hillier, W., Chen, H., Kordbacheh, F., Price, G.D., Djordjevic, M.A., 2011. Fatty acid profiling of *Chlamydomonas reinhardtii* under nitrogen deprivation. Bioresource Technology 102, 3343–3351.
Jones, C.S., Mayfield, S.P., 2012. Algae biofuels: versatility for the future of bioenergy. Current Opinion in Biotechnology 23, 346–351.
Kell, D.B., Markx, G.H., Davey, C.L., Todd, R.W., 1990. Real-time monitoring of cellular biomass: methods and applications. Trends in Analytical Chemistry 9, 190–194.
Kirby, B., 2010. Micro- and Nanoscale Fluid Mechanics: Transport in Microfluidic Devices. Cambridge University Press.
Maskow, T., Röllich, A., Fetzer, I., Ackermann, J.U., Harms, H., 2008. On-line monitoring of lipid storage in yeasts using impedance spectroscopy. Journal of Biotechnology 135, 64–70.
Mata, T.M., Martins, A.A., Caetano, N.S., 2010. Microalgae for biodiesel production and other applications: a review. Renewable and Sustainable Energy Reviews 14, 217–232.
Maxwell, E.N., 2007. Ultra-wideband electronics, design methods, algorithms, and systems for dielectric spectroscopy of isolated B16 tumor cells in liquid medium, Ph.D. thesis, University of South Florida, Department of Electrical Engineering.
Mourant, J.R., Yamada, Y.R., Carpenter, S., Dominique, L.R., Freyer, J.P., 2003. FTIR spectroscopy demonstrates biochemical differences in mammalian cell cultures at different growth stages. Biophysical Journal 85, 1938–1947.
Pal, D., Khozin-Goldberg, I., Cohen, Z., Boussiba, S., 2011. The effect of light, salinity, and nitrogen availability on lipid production by Nannochloropsis sp. Applied Microbiology and Biotechnology 90, 1429–1441.
Pozar, D.M., 2012. Microwave Engineering, fourth ed. John Wiley & Sons.
Pruvost, J., Vooren, G.V., Cogne, G., Legrand, J., 2009. Investigation of biomass and lipids production with *Neochloris oleoabundans* in photobioreactor. Bioresource Technology 100, 5988–5995.
Rodolfi, L., Zittelli, G.C., Bassi, N., Padovani, G., Biondi, N., Bonini, G., Tredici, M.R., 2008. Microalgae for oil: strain selection, induction of lipid synthesis and outdoor mass cultivation in a low-cost photobioreactor. Biotechnology and Bioengineering 102, 100–112.
Stephenson, A.L., Kazamia, E., Dennis, J.S., Howe, C.J., Scott, S.A., Smith, A.G., 2010. Life-cycle assessment of potential algal biodiesel production in the United Kingdom: a comparison of raceways and air-lift tubular bioreactors. Energy Fuels 24, 4062–4077.
Sturm, B.S.M., Lamer, S.L., 2011. An energy evaluation of coupling nutrient removal from wastewater with algal biomass production. Applied Energy 88, 3499–3506.
Sun, T., Gawad, S., Bernabini, C., Green, N.G., Morgan, H., 2007. Broadband single cell impedance spectroscopy using maximum length sequences: theoretical analysis and practical considerations. Measurement Science and Technology 18, 2859–2868.
Velmurugan, N., Sung, M., Yim, S.S., Park, M.S., Yang, J.W., Jeong, K.J., 2013. Evaluation of intracellular lipid bodies in *Chlamydomonas reinhardtii* strains by flow cytometry. Bioresource Technology 138, 30–37.
Wu, Y., Huang, C., Wang, L., Miao, X., Xing, W., Cheng, J., 2005. Electrokinetic system to determine differences of electrorotation and traveling-wave electrophoresis between autotrophic and heterotrophic algal cells. Colloids and Surfaces A: Physicochemical Engineering Aspects 262, 57–64.
Zhao, K., Bai, W., Mi, H., 2006. Dielectric spectroscopy of Anabaena 7120 protoplast suspensions. Bioelectrochemistry 69, 49–57.